Self-expandable hydrogel biliary stent design utilizing the swelling property of poly(vinyl alcohol) hydrogel

Self-expandable hydrogel biliary stent design utilizing the swelling property of poly(vinyl alcohol) hydrogel

Yoshiyasu Nagakawa[1,2]*, Satoshi Fujita[2,3]*, Shunji Yunoki[1], Takayoshi Tsuchiya[4], Shin-ichiro Suye[2,3], Takao Itoi[4]

[1] Biotechnology Group, Tokyo Metropolitan Industrial Technology Research Institute, 2-4-10, Aomi, Koto-ku, Tokyo, 135-0064, Japan

[2] Department of Frontier Fiber Technology and Sciences, Graduate School of Engineering University of Fukui, 3-9-1, Bunkyo, Fukui, 910-8507, Japan

[3] Life Science Innovation Center, University of Fukui, 3-9-1, Bunkyo, Fukui, 910-8507, Japan

[4] Department of Gastroenterology and Hepatology, Tokyo Medical University, 6-7-1, Nishishinjuku, Shinjuku-ku, Tokyo, Japan

Correspondence to: Yoshiyasu Nagakawa (E-mail: nagakawa.yoshiyasu@iri-tokyo.jp); Satoshi Fujita ((E-mail: fujitas@u-fukui.ac.jp))

ABSTRACT

We have developed a novel self-expandable biliary stent comprising poly(vinyl alcohol) (PVA). The swelling ratio of the dried PVA hydrogels decreased from 6.7 to 2.6 as the saponification degree increased from 95 to 99.9, whereas the storage modulus and tear strength increased from 17 to 400 kPa and from 0.5 to 10 N mm^{-1}, respectively. The dimensional ratios of the inner- and outer-diameter, and the length of the dried tube-shaped hydrogels (saponification degree of 98.5) prepared by simple air drying isotropically increased 1.4–1.5 times in physiological saline. Meanwhile, the dimensional ratios of the dried hydrogels prepared by drying under extension increased by twice, whereas the length decreases slightly, indicating anisotropic swelling. The radial force of the reswollen tube-shaped hydrogels (6.6 ± 0.6 mN mm^{-2}) was significantly higher than that of a conventional metallic stent (4.4 ± 0.3 mN mm^{-2}), suggesting that PVA hydrogels were applicable as self-expandable stents.

INTRODUCTION

Endoscopic biliary stenting is currently the standard palliative treatment for bile duct obstruction associated with malignant hepatobiliary tumors or benign strictures.[1-3] This stenting technique is a minimally invasive therapy compared to the surgical and percutaneous or nasobiliary drainage approaches, thereby improving the quality of life and the activities of daily living for patients.[4,5] Two types of stents have been employed in this technique and commercially available: self-expandable metallic stents (SEMSs) and plastic stents (PSs).[6-8] These stents, with different mechanical characteristics, are applied depending upon the bile duct symptoms.

The SEMS is a tubular mesh composed of shape-memory alloy (mainly nitinol),[6-8] which is accommodated in a narrow outer sheath of the endoscopic delivery system with a diameter of 8.5 Fr or less, where 1 Fr = 1/3 mm. After the stent is delivered into the bile duct via an endoscopic surgical access channel, it is released from the delivery system by withdrawing the outer sheath. The stent immediately self-expands in the duct to larger diameters ranging from 6–10 mm because of the property of the shape-memory alloy, enabling higher bile-flow rates with a later onset of clogging which result in longer patency compared to PSs.[9-11] However, SEMSs are more expensive and difficult to reposition after deployment.[12] Furthermore, the major problem associated with SEMS usage is tumor ingrowth or benign hyperplasia throughout the metal mesh voids leading to stent obstruction which render removal difficult and necessitate endoscopic reintervention.[13,14] On the other hand, the PS is a simple plastic tube composed of synthetic polymers such as polytetrafluoroethylene, polyethylene, or polyurethane. It can be removed and repositioned easily and is inexpensive compared to the SEMS.[12] However, the PS does not exhibit self-expandability and its diameter (up to 3.3 mm) is significantly lower than that of the SEMS, leading to occlusion within a shorter duration due to sludge or stone formation.[15,16] Therefore, the development of a self-expandable stent that can be removed from or repositioned in the bile duct is necessary.

We focus on the swelling property of the hydrogel to achieve self-expandability as well as removability. Hydrogels are generally composed of polymer networks among which aqueous solutions are confined. If the aqueous solutions are removed from hydrogels while maintaining their network structure, the obtained dried gel (i.e. xerogel) acquires the capacity to absorb aqueous solutions extensively, resulting in the dimensional expansion of the gel.[17] This physical property has been previously used for tissue expansion materials.[18,19] Therefore, for self-expandable stents, we apply the swelling property of tube-shaped hydrogels whose diameter enlarges in aqueous environment. A synthetic hydrophilic polymer, poly(vinyl alcohol) (PVA), is investigated for this purpose because it forms a hydrogel with excellent mechanical properties and long-term dimensional stability through simple physical cross-linking techniques.[20-22]

Moreover, PVA has been proved biologically safe because it has been used in numerous biomedical applications,[23,24] including wound dressings,[25,26] contact lenses,[27] and implants for various tissues and organs such as cartilage,[28] vascular access,[29] ligament,[30] and bone tissue engineering applications.[31]

In this study, we investigate the self-expandable properties of tube-shaped PVA hydrogels for assessing their potential application as novel self-expandable biliary stents. The fabrication conditions are optimized based on the swelling and mechanical test data of PVA hydrogel specimens. Dried tube-shaped PVA hydrogels rapidly swell and expand in physiological saline, and the inner diameter increases from 2.4 mm to 4.8 mm. Tube-shaped PVA hydrogels exhibit higher expansion force compared to conventional SEMSs, suggesting they can be applied as self-expandable stents.

EXPERIMENTAL

Materials

Four types of PVA powders were provided by Kuraray Co., Ltd. (Tokyo, Japan): Grade Nos. PVA-217, PVA-617, PVA-117, and PVA-HC. The respective saponification degrees were 88.0–89.0, 94.5–95.5, 98.0–99.0, and >99.85 mol% as per the manufacture's specifications; these powders are designated here as PVA-88, PVA-95, PVA-98.5, and PVA-99.9, respectively. The polymerization degree of all the grades was 1,700. Guaranteed reagent grades of sodium sulfate (Na_2SO_4; Wako Pure Chemical Industries, Osaka, Japan) and sodium chloride (NaCl; Wako Pure Chemical Industries, Osaka, Japan) were purchased and used without further purification. Commercialized SEMSs were purchased: Niti-S biliary covered stents (diameter: 6 mm and length: 100 mm; M. I. Tech Co., Ltd., Gyeonggi-do, Korea) and Hanaro biliary covered stents (diameter: 6 mm and length: 100 mm; Taewoong Medical Co., Ltd., Gyeonggi-do, Korea).

Preparation of PVA hydrogels

PVA hydrogels with various shapes were prepared from the solution by conventional freezing/thawing treatment. In brief, each of the PVA powders was dissolved in hot water (100 °C) at a concentration of 10 w/w%. Sodium sulfate solution (2 M) was gradually added to the PVA solution under agitation to achieve a final concentration of 0.45 M, resulting in the precipitation of PVA.[32] The precipitated PVA was placed in a 50 mL tube and centrifuged at 4,500 rpm for 3 min to obtain a dense precipitate without air bubbles, and then poured into two types of molds: disc-shaped (biological dish with 50-mm diameter and 2–3-mm thickness) and custom-made tube-shaped molds (polytetrafluoroethylene; length: 80 mm, inner diameter: 5mm, and outer

diameter: 8mm). The molds were placed in a freezer and subjected to freezing/thawing treatment involving a cycle of freezing (−30 °C for 12 h) and subsequent thawing (25 °C for 1 h), producing disc-shaped and tube-shaped PVA hydrogels. Rectangular-shaped PVA hydrogels were cut from the disc-shaped hydrogels.

Dried hydrogel specimens were prepared from the three types of PVA hydrogels for swelling tests. Dried disc-shaped and rectangular hydrogel specimens were obtained by drying to a constant weight at 60 °C in a dry oven. Dried tube-shaped hydrogel specimens were fabricated from the tube-shaped PVA hydrogels by drying under extension. Both ends of the hydrogels were penetrated with silk strings. Each of the hydrogels was placed vertically in a drying chamber (600 mm × 500 mm × 500 mm) at 60°C under tension: one end of the hydrogel was anchored to the ceiling of the chamber with the string and the other end was connected with weights (approximately 1 kg) to achieve a certain extension (1.7 folds in length). After drying, both the ends of the hydrogel (approximate length 25 mm) were cut from the specimen to remove the penetrated parts. The dried tube-shaped hydrogel specimens without extension were also prepared from the tube-shaped PVA hydrogels without using weights. The sizes of PVA hydrogels decreased by drying process. As a result, dried tube-shaped PVA hydrogels under extension (length: 85 mm, inner diameter: 2.4 mm, and outer diameter: 3.7 mm) and without extension (length: 35 mm, inner diameter: 3.5 mm, and outer diameter: 5.5 mm) were obtained. The dimensional changes due to swelling were tested for both types of dried tube-shaped hydrogel specimen.

Reswollen disc-shaped and rectangular hydrogel specimens were prepared from the corresponding dried specimens by swelling in physiological saline. The reswollen specimens were subjected to the mechanical and structural evaluation tests described below. Reswollen tube-shaped hydrogel specimens were obtained at the same condition from the reswollen disc-shaped and rectangular hydrogels, and subjected to the radial force test.

Swelling properties of dried-state PVA hydrogels

Free swelling tests. The water absorbability of dried PVA hydrogels was evaluated by swelling, by a modified version of a previous method.[21] Briefly, the dried rectangular hydrogel specimens were immersed in 0.9% NaCl (i.e., physiological saline) at 37 °C for 3, 6, 12, 24, 48, 72, and 96 h. The swelling property of dried PVA hydrogels was calculated as the ratio of the weights or volumes before (W_d or V_d) and after swelling (W_s or V_s).

Swelling tests under controlled expansion force. The swelling of dried PVA hydrogels was monitored using a texture analyzer (TA. XTplus; Stable Micro Systems, Godalming, UK) under a controlled expansion force at 37°C. The dried disc-shaped specimen (diameter: 10mm, thickness:

2–4 mm) was placed in the center of a glass dish (diameter: 90 mm, depth: 20 mm). The circular probe (diameter: 60 mm) of the texture analyzer was contacted with the upper surface of the specimen, where the vertical force was mechanically controlled at 1.6 N. When the elastic modulus of healthy human bile duct (1.3 kPa[33]) is assumed to increase by the development of cancer in the same manner as for fibrosis of human liver (from 2 to 20 kPa),[34] the modulus of human bile duct which develops cancer is estimated to be less than 20 kPa. This stress can be converted to 1.6 N for the disc-shaped hydrogel specimen (diameter 10 mm), which corresponds to the force for expanding human bile duct which develops cancer by at least twice. Physiological saline was then poured onto the glass dish to a level higher than the circular probe, causing the specimen to swell. While the vertical force against the probe (i.e. expansion force) was maintained, the specimen gradually expanded, causing the probe to rise; this increase in distance was continuously recorded for 80 h. The swelling under controlled expansion force was expressed as the ratio of the sample heights before and after swelling.

Characterization of reswollen PVA hydrogels

Dynamic viscoelastic measurements. The shear storage modulus (*G´*) was measured at room temperature through dynamic viscoelastic measurements with a parallel-plate rheometer (MCR302; Anton Paar, Graz, Austria), by a slightly modified version of a previous method.[26] The disc-shaped specimen was placed on the bottom plate of the rheometer, and then the upper plate (diameter: 25 mm) was moved to contact with the specimen, after which oscillatory frequency sweep (frequency: 0.01–10 Hz, strain 0.1 %) was conducted. *G´* at a frequency of 1 Hz was employed because it did not exhibit frequency dependency at frequencies near 1 Hz.

Tear tests. The tear strengths were measured using the texture analyzer equipped with a tensile grip. Both ends of each rectangular specimen were penetrated with metal hooks (diameter: 1 mm) fixed to the tensile grip. The specimen was elongated longitudinally at a cross-head speed of 1 mm s^{-1}. The tear strength (N mm^{-1}) was obtained from the load at the breaking point by subtracting the gel thickness.

Repeated compression tests. The hysteresis loops were obtained at room temperature using the texture analyzer equipped with a circular probe (diameter: 20 mm), by a slightly modified version of a method described in a previous report.[35] Briefly, the disc-shaped specimen (diameter: 10 mm, thickness: 3–6 mm) was compressed at a cross-head speed of 0.5 mm s^{-1} to achieve strain of 20 %, and immediately returned to the initial position. The tests were repeated 10 times.

Crystallinity estimation. Wide-angle X-ray diffraction (WAXD) measurements were performed on the disc-shaped specimens with a X-ray diffractometer (Rigaku SmartLab, Tokyo, Japan) using

Ni-filtered Cu Kα rays at 40kV and 30 mA, scanning at 3 deg min^{-1} in the 2θ range of 10°–60°, described in previous reports.[36,37]

Evaluation of tube-shaped hydrogels as a self-expandable stent

Dimensional change by swelling. The sizes (inner-diameter, outer-diameter, and length) of tube-shaped hydrogels without and with extension were measured with a caliper, these hydrogels were then immersed in physiological saline at 37 °C for over 96 h. After immersion, the sizes of the reswollen tube-shaped hydrogels were measured. The dimensional changes were expressed as the ratio of the sizes before and after swelling.

Radial force tests. The radial force was tested using the texture analyzer described in the JIS T 0401 standard,[38] as shown in Scheme 1. Briefly, a polypropylene film (thickness: 30 μm) was alternately wound onto the sample, and perpendicularly elongated at a test speed of 0.08 mm s^{-1}; the force was measured until the initial sample diameter (D_0) [mm] became $0.8D_0$. The distance of the grip at $0.8D_0$ (M) [mm] was calculated using equation (1):

$$M = 0.2D_0\pi \quad (1)$$

The surface area after elongation (S) [mm^2] was calculated using equation (2):

$$S = 0.8D_0\pi L \quad (2)$$

where L [mm] is the length of the film wound onto the samples. The radial force (P) [N mm^{-2}] was calculated using equation (3):

$$P = F / S \quad (3)$$

where F [N] is the stress with the elongation at $0.8D_0$.

Statistics

All these test data were presented as the mean ± standard deviation (SD) (n = 3). Data from the radial force tests were compared individually using one-way variance analysis. Significant differences between the groups were calculated using one-way variance analysis followed by Tukey's test ($p < 0.05$).

RESULTS

Effect of the saponification degree on the swelling and mechanical properties of PVA hydrogels

Swelling properties in the unconstrained condition

The W_s/W_d values of dried PVA hydrogels increased in a time-dependent manner (Figure 1(a)). The W_s/W_d values of PVA-98.5 and PVA-99.9 sharply increased at the beginning of the immersion in physiological saline at 37 °C, and reached a plateau after 24-h of immersion. On the other hand, a continuous increase in W_s/W_d was observed after 72-h of immersion for PVA-95. Dried PVA-88 hydrogel was excluded from the swelling tests because the specimens dispersed after immersion into physiological saline. The swelling properties increased as the saponification degree decreased (Figure 1). Dried PVA-95 hydrogel exhibited the highest W_s/W_d throughout the immersion period, and the plateaued W_s/W_d was 6.7 ± 0.3. The plateaued W_s/W_d of PVA-98.5 (3.2 ± 0.1) was higher than that of PVA-99.9 (2.6 ± 0.01). In addition to evaluating W_s/W_d, the increase in volume (V_s/V_d) was calculated. The trend of the plateaued V_s/V_d values with respect to the saponification degree of PVA were similar to those of the W_s/W_d values (Figure 1(b)), indicating that the V_s/V_d values of PVA hydrogels increase in conformity with the W_s/W_d values. As PVA-88 dispersed in physiological saline, our observations were focused on PVA-95, PVA-98.5, and PVA-99.9.

Relationship between the saponification degree and mechanical properties

Figure 2(a) shows the results of the dynamic viscoelastic measurements of the three types of reswollen disc-shaped PVA hydrogels. The G´ of each specimen was almost constant in the frequency range 0.05–3 Hz, where the G´ was the following order: PVA-99.9 > PVA-98.5 > PVA-95. Tanδ of the reswollen hydrogels (<0.05) were much lower than 1, suggesting the elasticities typical in cross-linked polymer hydrogels. Similar trends were observed for the tear strengths of reswollen PVA hydrogels (Figure 2(b)). As the saponification degree increased, the tear strength of reswollen hydrogels increased, while the elongation at break points were comparable for the three types of specimens. The elasticities were further examined by the repeated compression tests (Figure 2(c)–(e)). The stress–strain relationships in 10 times repeated compression were almost constant for each of the reswollen hydrogels, indicating rubber-like elasticities against compression.

G´ and tear strengths were plotted against the saponification degree and W_s/W_d values (Figure 2(f) and (g)). The reswollen PVA-99.9 hydrogel had the highest *G´* (400 ± 40 kPa). PVA-98.5 had a similar texture, but its *G´* was 260 ± 20 kPa which was lower than that of PVA-99.9. Although the results of loading-de-loading cycles indicated that PVA-95 showed rubber-like texture, it turned viscous with swelling. This softening reflected the least *G´* (17 ± 0.1 kPa). Corresponding results were obtained for the tear strengths of reswollen PVA hydrogels. The tear strengths of PVA-99.9, PVA-98.5, and PVA-95 were 10 ± 0.8 N mm^{-1}, 5.9 ± 0.5 N mm^{-1}, and 0.5 ± 0.02 N mm^{-1},

respectively. Figure 2(g) shows that G' and the tear strengths of the reswollen PVA hydrogels decrease exponentially with the increase in W_s/W_d values.

Figure 3 displays the X-ray diffraction patterns of the reswollen PVA hydrogels. The sharpest crystalline reflection in the 2θ range at 19.3° was observed in PVA-99.9; the peak value was consistent with that of a previous report.[36] The crystalline reflection decreased with the decrease in the saponification degree of PVA. PVA-95 exhibited almost no crystalline reflection peaks. The crystallinity of PVA-98.5 and PVA-99.9 were estimated to be 0.7 ± 0.05% and 1.6 ± 0.05 %, respectively. Due to solvent scattering, both crystallinity values were low, as previously reported.[36,37] The results of the mechanical tests demonstrated that the reswollen PVA-95 hydrogel was highly softened due to swelling; hence, PVA-95 was excluded from the following tests which were designed to evaluate the characteristics of PVA hydrogels for application as self-expandable biliary stents.

Swelling properties under controlled expansion force

The time-dependent swelling of dried PVA-98.5 and PVA-99.9 hydrogels was observed under a constant compression force (Figure 4). The swelling of both the dried hydrogels rapidly progressed immediately after immersion in physiological saline (0–6 h), after which the increase in the swelling ratios were moderate. The saturation was observed in 60 h-immersion. The ratio of the sample heights before and after swelling for both PVA-98.5 and PVA-99.9 was 1.3 ± 0.05. Therefore, PVA-98.5 hydrogel with good mechanical as well as swelling properties was subjected to the following tests for the tube-shaped hydrogels.

Potential of tube-shaped hydrogels for application as self-expandable biliary stents

Effect of the drying condition on dried tube-shaped hydrogels with extension

Figures 5(a)–(d) depict the representative appearances of dried tube-shaped hydrogels with and without extension before and after swelling. The ratios of the inner-diameter, outer-diameter, and length of these dried tube-shaped hydrogels before and after swelling are indicated by the dimensional ratios (Figure 5(e)). The dimensional ratios of tube-shaped hydrogels with extension were anisotropic: the ratios of the inner- and outer-diameters reached 2.0, while that of the length was only 0.78 ± 0.03 because of shortening due to swelling (Figure 5(a), (b), and (e)). The sizes of inner-diameter, outer-diameter, and length of the reswollen tube-shaped hydrogel with extension were 4.8 ± 0.2 mm, 7.8 ± 0.4 mm, and 61 ± 7 mm, respectively. In contrast, the dimensional ratios of tube-shaped hydrogels without extension were almost isotropic (ranging from 1.4–1.5); inner-diameter, outer-diameter, and length of reswollen hydrogel without extension were 5 mm, 8.5 mm, and 52 mm (error bound <0.1)), respectively. As the anisotropic swelling property with preferential increase in the inner- and outer diameters is advantageous

for application as a self-expandable biliary stent, the following radial force tests were conducted on reswollen tube-shaped PVA hydrogels with extension.

Radial-force comparison between tube-shaped PVA hydrogels and commercialized SEMSs

The radial forces of reswollen tube-shaped hydrogels and the two commercialized SEMSs are shown in Figure 6. The load of the two commercialized SEMSs linearly increased as the diameters were decreased by binding with plastic tape. On the other hand, the change in the load of reswollen tube-shaped hydrogels was divided into two regions: gently sloped (diameter reduction ratio: 0–0.05) and the subsequent steeply sloped region (diameter reduction ratio: 0.05–0.2) (Figure 6(a)). In accordance with the JIS T 0401 standard, the radial forces (N mm^{-2}) at a diameter reduction ratio of 0.2 for each stent were compared (Figure 6(b)). The radial force of reswollen tube-shaped hydrogels (6.6 ± 0.6 mN mm^{-2}) was significantly higher than those of the Niti-S (4.4 ± 0.3 N mm^{-2}) and Hanaro stents (3.6 ± 0.4 N mm^{-2}).

DISCUSSION

This is the first study that shows the potential of a self-expandable hydrogel stent with a capacity to expand by swelling. Swelling properties of polymer hydrogels are well known and have been applied for some industrial products such as disposable diapers[39]; however, no attempt has been made to utilize swelling properties for generating self-expansion forces of medical stents. In general, swelling of hydrogels is an unfavorable property because it decreases polymer densities and mechanical properties. The weakness of hydrogels after swelling is a limitation for biomedical applications.[40] However, we intended to use the swelling properties as an effectiveness of a medical device: self-expandability of stents. This study was thus designed based on the speculation that a polymer hydrogel with stiffness and hardness while having swelling properties generates self-expansion forces. We focused PVA as a polymer substrate of self-expandable stents because of the following favorable characteristics: physically cross-linkable properties by a simple freeze/thaw method, hardness and stiffness of the hydrogel obtained, and biological safety of the polymer. Physical crosslinking methods are preferable to chemical methods in terms of the risk of toxicity. In this study, the molecular structures of PVA and fabrication processes of stents were optimized to achieve self-expandability comparable to SEMSs while maintaining good mechanical properties. We evaluated the potential of cross-liked tube-shaped PVA hydrogels as a self-expandable biliary stent.

Swelling capacity is one of the substantial properties for designing self-expandable stents from dried PVA hydrogels. As shown in Figure 1, the unconstrained swelling property of dried PVA hydrogels increased as the saponification decreased. We further confirmed that the V_s/V_d values

of dried PVA-95, PVA-98.5, and PVA-99.9 hydrogels were in conformity with the W_s/W_d values (Figure 1(b)), indicating that these gels can swell in physiological saline without breakage of the gel structure except for dried PVA-88. Swelling properties of PVA hydrogels are affected by both crystallinity and cross-link density,[41] which depend on saponification degrees of PVA molecules. We intended to explain the effects of saponification on the swelling properties as well as on the mechanical properties in terms of crystallinity[21,22] because a freeze/thaw method grows crystalline of PVA which acts as cross-linking points. It is thus difficult to distinguish the mechanical contribution of crystallinity from that of crosslinking. It should also be noted that the crosslinking structures of PVA hydrogels obtained by a freeze/thaw method are different from those obtained by gamma-irradiation or chemical crosslinkers, in which PVA molecules are crosslinked with the absence of crystalline.

WAXD analyses of the reswollen PVA hydrogels showed the crystallinity increased as the saponification degree increased (Figure 3), which explains the saponification degree-dependence of the swelling properties of PVA hydrogels (Figure 1). This dependency was reported previously for PVA hydrogels fabricated by cast-drying method.[42] Although the reswollen PVA-95 hydrogel did not exhibit crystalline reflection peaks, this swollen hydrogel enabled gel formation, whereas PVA-88 could not form a gel structure and dispersed in physiological saline. PVA with lower saponification seems to have less capacity to grow crystalline and to form physical crosslinking, as shown in a previous report,[21] in which PVA film prepared by cast-drying method with saponification degree of 78–81 % completely dissolved into the water.

Swelling of hydrogels means decreases of polymer densities. Thus, we evaluated mechanical properties of reswollen hydrogels from PVA-99.9, PVA-98.5, and PVA-95 with different swelling capacities. The G' and tear strengths increased with increasing the saponification degree (Figure 2(f)) while showing a rubber-like elasticity (Figures 2(c)–2(e)). This saponification degree-dependence of the mechanical properties was opposite to that of the swelling properties, indicating that there is a tradeoff relationship between swelling properties of dried PVA hydrogels and mechanical properties after swelling, as mentioned by Suzuki and Sasaki.[42] (Figures 2(f) and 2(g)). In addition, the relationship could depend on crystallinity of PVA, according to the findings by Fukumori and Nakaoki.[22] Considering the free swelling and mechanical properties, PVA-98.5 and PVA-99.9 are applicable as a potential use of self-expandable biliary stents because their textures could be resistant to pulling with forceps (Figure 2b). Although PVA-95 exhibited the highest swelling property, its texture was viscous and fragile; hence, we determined that PVA-98.5 and PVA-99.9 are potentially applicable as self-expandable stents. The following tests were performed for the two hydrogels.

We devised the swelling test under controlled stress and evaluated the swelling of dried PVA-98.5 and PVA-99.9 hydrogels (Figure 4). The results suggested both the dried hydrogels had a capacity to expand bile ducts by swelling, because the controlled force corresponds to the force which can expand bile ducts by twice. The vertical force applied in the swelling tests under a controlled expansion force (20 kPa on the specimen) is close to the previously reported maximal value of the elastic modulus of the gastrointestinal tissue which varies widely (range: 0.6–20 kPa).[33,34,43,44] We set the controlled vertical force for the swelling tests based on the following facts and estimations. It has been reported that healthy human bile duct has an elastic modulus of approximately 1.3 kPa.[33] On the other hand, it has been reported that the elastic modulus of human liver increases from 2 kPa to 20 kPa by pathogenesis of fibrosis.[34] We thus assumed that the elastic modulus of human bile duct which develops cancer was as high as 20 kPa. This stress means the force to expand bile duct by twice, and the force on the hydrogel specimen (diameter 10 mm) was calculated to be 1.6 N.

Taking the results that the PVA-98.5 hydrogel showed good swelling and mechanical properties, we chose PVA-98.5 as a base polymer for the tube-shaped hydrogel as a self-expandable stent. The test for evaluating the effect of the drying condition demonstrated that dried tube-shaped PVA hydrogels with extension swelled anisotropically, whereas those without extension swelled isotropically (Figure 5). These results indicate that the dimensional ratios of the inner- and outer-diameter was increased by the effect of extension. Furthermore, the difference in the length dimensional ratios between tube-shaped hydrogels with and without extension suggest that the increase in length is transferred as increase in the inner- and outer- diameters. Although the anisotropic swelling mechanism of tube-shaped hydrogels was unknown, we speculate that anisotropic crystallization created by drying under extension played a crucial role on the characteristic swelling behavior. The PVA polymer chains of tube-shaped hydrogels with extension are stretched in a perpendicular direction. During the drying process, the structure of the stretched polymer chains is preserved in the dried-state, including nonstretched chains to some extents. The ratio of the stretched and nonstretched PVA chains involves the degree of anisotropic swelling of the PVA hydrogel.

We employed only the tube-shaped hydrogel with extension for the radial force tests because the hydrogels without extension showed unfavorable lengthening. Clinicians in gastrointestinal medicine regard self-expandable stents exhibiting large shortening or lengthening not useful in clinical applications. The expansion force of the conventional SEMS is referred to as the radial force and is considered critical for expanding the luminal patency at the stricture.[45,46] The higher radial force of reswollen PVA-98.5 hydrogel compared to those of the commercialized SEMSs would be sufficient for expanding the tissue (Figure 6(b)). The load curve of tube-shaped hydrogels seemed to exhibit the J- curve, whereas linearly increasing curves are observed for the

Niti-S and Hanaro stents (Figure 6(a)). It was reasonable that the load curve of SEMSs linearly increased as the inner diameter shrank because they exhibit a spring-like self-expanding property; on the other hand, the self-expanding property of the PVA hydrogel-based stent is initiated by the swelling property. This might have caused the differences in the load curves of tube-shaped hydrogels and SEMSs. It is reasonable to assume that dried tube-shaped hydrogels initiate the self-expanding property by swelling in the fluid after deployment in the bile duct.

We measured the radial force of reswollen tube-shaped hydrogel which was completely swollen with physiological saline. Therefore, our radial force investigation could not evaluate the expansion force from the initial drying to the swelling of tube-shaped PVA hydrogels. However, JIS T 0401 recommends the evaluation of the radial force at 0.8 times the completely expanded diameter, indicating that the radial force toward the end of expansion is important. Swelling can be considered complete when the diameter of the tube-shaped PVA hydrogel is 0.8 times the completely expanded diameter. Hence, it can be assumed that our observation evaluates the radial force of the tube-shaped hydrogel toward the end of the expansion, i.e. when the swelling is almost complete. Considering the J-curve-like increase in the load and the higher radial force compared to commercialized SEMSs, tube-shaped hydrogels have sufficient force to expand the biliary tract. In vivo evaluation of the tube-shaped PVA hydrogels as self-expandable biliary stents is in progress.

CONCLUSIONS

We developed a novel hydrogel-based self-expandable biliary stent comprising PVA hydrogel formed in conjunction with salt modified and the freeze/thaw cross-linking method, with sufficient mechanical and anisotropic swelling properties. Saponification degree was the predominant factor for designing a self-expandable stent from PVA hydrogel which inversely affects mechanical properties and swelling properties. PVA-98.5 appeared to be most preferable to self-expandable stent applications among PVA with different saponification degrees. The radial force of the reswollen tube-shaped PVA-98.5 hydrogel was higher than those of conventional SEMSs, indicating that PVA hydrogel-based stents are potentially applicable as self-expandable biliary stents. Moreover, PVA is inexpensive and safe, and the method for preparing the PVA hydrogels is simple. Thus, PVA hydrogel-based self-expandable stents are suitable for practical application.

ACKNOWLEDGEMENTS

This work was partly supported by the Japan Society for the Promotion of Science (JSPS) [Grants-in-Aid for Scientific Research (C) No. 18K07954]. The authors would like to thank Kuraray Co., Ltd. for kindly providing the PVA samples, Dr. Kiyoji Sugimoto (Tokyo Metropolitan Industrial Technology Research Institute) for his fruitful advice on the rheological experiment, Dr. Daisuke Ogawa (Tokyo Metropolitan Industrial Technology Research Institute) for his helpful advice on the WAXD measurement, and Editage (www.editage.jp) for the English language review.

REFERENCES

1. Itoi, T.; Itokawa, F.; Sofuni, A.; Kurihara, T.; Ishii, K.; Tsuji, S.; Ikeuchi, N.; Umeda, J.; Tanaka, R.; Tonozuka, R.; Moriyasu, F. *Endosc. Ultrasound*. **2012,** *1*, 36.

2. Kato, H.; Tsutsumi, K.; Kawamoto, H.; Okada, H. *World J. Gastrointest. Endosc.* **2015,** *7*, 1032.

3. Kawakami, H.; Itoi, T.; Kuwatani, M.; Kawakubo, K.; Kubota, Y.; Sakamoto, N. *J. Hepatobiliary Pancreat. Sci.* **2015,** *22*.

4. Soehendra, N.; Reynders-Frederix, V. *Endoscopy*. **1980,** *12*, 8.

5. Ballinger, A.; McHugh, M.; Catnach, S.; Alstead, E.; Clark, M. *Gut*. **1994,** *35*, 467.

6. Mangiavillano, B.; Pagano, N.; Baron, T. H.; Arena, M.; Iabichino, G.; Consolo, P.; Opocher, E.; Luigiano, C. *World J. Gastrointest. Endosc.* **2016,** *8*, 143.

7. Dumonceau, J.-M.; Heresbach, D.; Devière, J.; Costamagna, G.; Beilenhoff, U.; Riphaus, A. *Endoscopy*. **2011,** *43*, 617.

8. Pfau, P. R.; Pleskow, D. K.; Banerjee, S.; Barth, B. A.; Bhat, Y. M.; Desilets, D. J.; Gottlieb, K. T.; Maple, J. T.; Siddiqui, U. D.; Tokar, J. L. *Gastrointest. Endosc.* **2013,** *77*, 319.

9. Liberato, M. J. A.; Canena, J. M. T. *BMC Gastroenterol.* **2012,** *12*, 103.

10. Sangchan, A.; Kongkasame, W.; Pugkhem, A.; Jenwitheesuk, K.; Mairiang, P. *Gastrointest. Endosc.* **2012,** *76*, 93.

11. Itoi, T.; Sofuni, A.; Itokawa, F.; Tonozuka, R.; Ishii, K. *Dig. Endosc.* **2013,** *25*, 63.

12. Itoi, T.; Isayama, H.; Sofuni, A.; Itokawa, F.; Kurihara, T.; Tsuchiya, T.; Tsuji, S.; Ishii, K.; Ikeuchi, N.; Tanaka, R. *J. Hepatobiliary Pancreat. Sci.* **2011,** *18*, 664.

13. Vakil, N.; Morris, A. I.; Marcon, N.; Segalin, A.; Peracchia, A.; Bethge, N.; Zuccaro, G.; Bosco, J. J.; Jones, W. F. *Am. J. Gastroenterol.* **2001,** *96*, 1791.

14. Isayama, H.; Komatsu, Y.; Tsujino, T.; Sasahira, N.; Hirano, K.; Toda, N.; Nakai, Y.; Yamamoto, N.; Tada, M.; Yoshida, H. *Gut*. **2004,** *53*, 729.

15. Hoffman, B. J.; Cunningham, J. T.; Marsh, W. H.; O'Brien, J. J.; Watson, J. *Gastrointest. Endosc.* **1994,** *40*, 581.

16. Kwon, C. I.; Lehman, G. A. *Clin. Endosc*. **2016,** *49*, 139.

17. Stauffer, S. R.; Peppas, N. A. *Polymer*. **1992,** *33*, 3932.

18. Wiese, K. *J. Craniomaxillofac. Surg.* **1993,** *21*, 309.

19. Swan, M.; Bucknall, D.; Goodacre, T.; Czernuszka, J. *Acta Biomater.* **2011,** *7*, 1126.

20. Hassan, C. M.; Peppas, N. A. *Macromolecules*. **2000,** *33*, 2472.

21. Otsuka, E.; Suzuki, A. *J. Appl. Polym. Sci.* **2009,** *114*, 10.

22. Fukumori, T.; Nakaoki, T. *J. Appl. Polym. Sci.* **2014,** *131*.

23. Muppalaneni, S.; Omidian, H. *J. Dev. Drugs*. **2013,** *2*.

24. Wan, W.; Bannerman, A. D.; Yang, L.; Mak, H. In Polymeric Cryogels; Springer, 2014.

25. Kokabi, M.; Sirousazar, M.; Hassan, Z. M. *Eur. Polym. J.* **2007,** *43*, 773.

26. Yunoki, S.; Kohta, M.; Ohyabu, Y.; Sekiguchi, M.; Kubo, T.; Iwasaki, T. *J. Appl. Polym. Sci.* **2014,** *131*.

27. Hyon, S.-H.; Cha, W.-I.; Ikada, Y.; Kita, M.; Ogura, Y.; Honda, Y. *J. Biomater. Sci. Polym. Ed.* **1994,** *5*, 397.

28. Baker, M. I.; Walsh, S. P.; Schwartz, Z.; Boyan, B. D. *J. Biomed. Mater. Res. Part B*. **2012,** *100*, 1451.

29. Negishi, J.; Nam, K.; Kimura, T.; Hashimoto, Y.; Fusamoto, S.; Higami, T.; Fujisato, T.; Kishida, A. *J. Biomed. Mater. Res. Part B*. **2014,** *102(7)*, 1426.

30. Moreau, D.; Villain, A.; Bachy, M.; Proudhon, H.; Ku D.-N.; Hannouche, D.; Petite, H.; Corté, L. *J. Mater. Sci. Mater. Med.* **2017**, *28*, 114.

31. Hou. Y.; Xie, W.; Achazi, K.; Cuellar-Camacho, J.-L.; Melzig, M. F.; Chen, W,; Haag, R. *Acta Biomater.* **2018,** *77*, 28.

32. Curley, C.; Hayes, J. C.; Rowan, N. J.; Kennedy, J. E. *J. Mech. Behav. Biomed. Mater.* **2014,** *40*, 13.

33. Li, W.; Zhang, H.; Li, J.; Dong, R.; Yao, B.; He, X.; Wang, H.; Song, J. *Transplant. Proc.* **2013**, *45*, 741.

34. Yeh, W.-C.; Li, P.-C.; Jeng, Y.-M.; Hsu, H.-C.; Kuo, P.-L.; Li, M.-L.; Yang, P.-M.; Lee, P. H. *Ultrasound Med. Biol.* **2002,** *28*, 467.

35. Yunoki, S.; Ikoma, T.; Monkawa, A.; Marukawa, E.; Sotome, S.; Shinomiya, K.; Tanaka, J.; *J. Biomater. Sci. Poly. Edn.* **2007,** *18*, 393

36. Ricciardi, R.; Auriemma, F.; De Rosa, C.; Lauprêtre, F. *Macromolecules*. **2004,** *37*, 1921.

37. Ricciardi, R.; Auriemma, F.; Gaillet, C.; De Rosa, C.; Lauprêtre, F. *Macromolecules*. **2004,** *37*, 9510.

38. Committee, J. I. S. *Japanese Standards Association*. **2013**.

39. Ahmed, E. M. *J. Adv. Res*. **2015,** *6*, 105.

40. Kamata, H.; Akagi, Y.; Kayasuga-Kariya, Y.; Chung, U.-i.; Sakai, T. *Science*. **2014,** *343*, 873.

41. Urushizaki, F.; Yamaguchi, H.; Nakamura, K.; Numajiri, S.; Sugibayashi, K.; Morimoto, Y. *Int. J. Pharm.* **1990,** *58*, 135

42. Suzuki, A.; Sasaki, S. *Proc. Inst. Mech. Eng. H*. **2015,** *229*, 828.

43. Inoue, Y.; Kokudo, N. *Surg. Today*. **2014,** *44*, 1793.

44. Garteiser, P.; Doblas, S.; Daire, J.-L.; Wagner, M.; Leitao, H.; Vilgrain, V.; Sinkus, R.; Van Beers, B. E. *Eur. Radiol.* **2012,** *22*, 2169.

45. Isayama, H.; Nakai, Y.; Toyokawa, Y.; Togawa, O.; Gon, C.; Ito, Y.; Yashima, Y.; Yagioka, H.; Kogure, H.; Sasaki, T.; Arizumi, T.; Matsubara, S.; Yamamoto, N.; Sasahira, N.; Hirano, K.; Tsujino, T.; Toda, N.; Tada, M.; Kawabe, T.; Omata, M. *Gastrointest. Endosc.* **2009,** *70*, 37.

46. Isayama, H.; Nakai, Y.; Hamada, T.; Matsubara, S.; Kogure, H.; Koike, K. *Curr. Gastroenterol. Rep.* **2016,** *18*, 64.

Captions

Scheme 1. Schematic illustration of the radial force test method. Tube-shaped PVA hydrogel or SEMS (a) was wound onto polypropylene film (b) and gripped with the upper and lower sensors (c_1 and c_2). The test sample was perpendicularly elongated (d) until the initial diameter (D_0) became $0.8D_0$ (e).

Figure 1. Free swelling behavior of dried PVA hydrogels. (a) Change of W_s/W_d as a function of immersion time in physiological saline at 37 °C. (b) Comparison between saturated V_s/V_d and W_s/W_d. Data are presented as the mean ± SD (n=3).

Figure 2. Effect of saponification on mechanical properties of reswollen PVA hydrogels. (a) Shear storage modulus (G') and loss tangent (tanδ) of PVA-95 (circles), PVA-98.5 (triangles), and PVA-99.9 (squares) as a function of frequency. Closed and open symbols indicate G' and tanδ, respectively. (b) Typical load-deformation curves of the hydrogels obtained by tear tests. (c)–(e) Typical loading-de-loading cycles (hystereses) for PVA-95 (c), PVA-98.5 (d), and PVA-99.9 (e) obtained by repeated compression tests. (f), (g) Shear storage modulus and tear strength of the hydrogels as a function of saponification degree (f) and W_s/W_d (g). The storage modulus of PVA-95, PVA-98.5, and PVA-99.9 are denoted by open circles, triangles, and squares, respectively (left vertical axis). The tear strengths of PVA-95, PVA-98.5, and PVA-99.9 are denoted by closed circles, triangles, and squares, respectively (right vertical axis). Data are presented as the mean ± SD (n=3). All the data contained experimental errors, but the error bars in some data are so small that they are included in each symbols.

Figure 3. WAXD patterns of reswollen PVA hydrogels.

Figure 4. Temporal change in the height ratios before and after swelling of dried PVA-98.5 (open circles) and PVA-99.9 (closed circles) hydrogels.

Figure 5. Effects of extension during drying process of tube-shaped PVA hydrogels on swelling behaviors. (a, b) Representative appearances of tube-shaped hydrogels with extension (a, front view; b, top view). It can be seen that the diameter of the dried tube-shaped hydrogel (left in (a)) was expanded by swelling (right in (a)). In contrast, the length of the dried tube-shaped hydrogel (upper in (b)) was shortened by swelling (lower in (b)). (c, d) Representative appearances of tube-shaped hydrogels without extension (c, front view; d, top view). The diameter and length of the dried tube-shaped PVA hydrogel (left in (c); upper in (d)) were expanded by swelling at a same dimensional ratio. (e) Dimensional ratios of the inner diameter (I.D.), outer diameter (O.D.), and length of tube-shaped PVA hydrogels without extension (closed bars) and with extension (open bars) before and after swelling. Data are presented as the mean ± SD (n=3).

Figure 6. Results of radial force tests of reswollen tube-shaped PVA-98.5 hydrogel and commercialized SEMSs. (a) Typical load-deformation curves. The deformations were shown as diameter reduction ratios. (b) Radial forces of the three stents at a diameter reduction ratio of 0.2. Data are presented as the mean ± SD (n=3). * $p < 0.05$.

Scheme 1

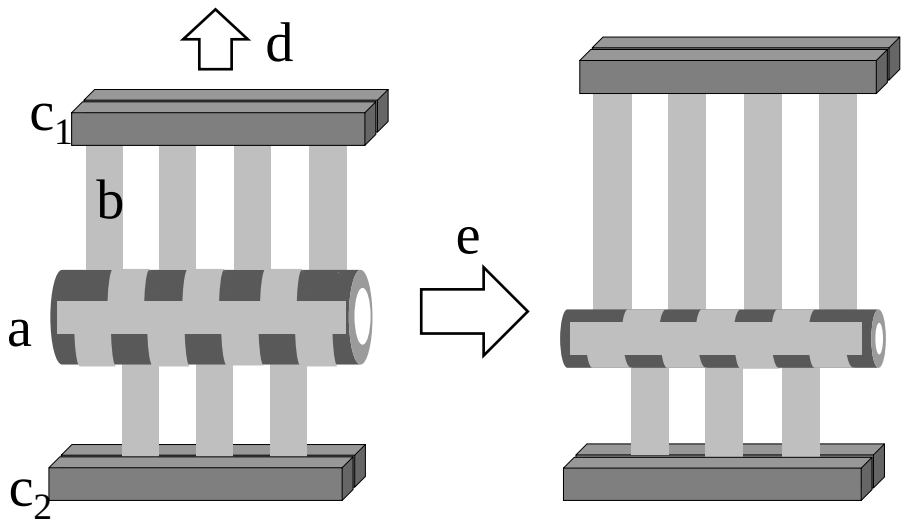

Figure 1

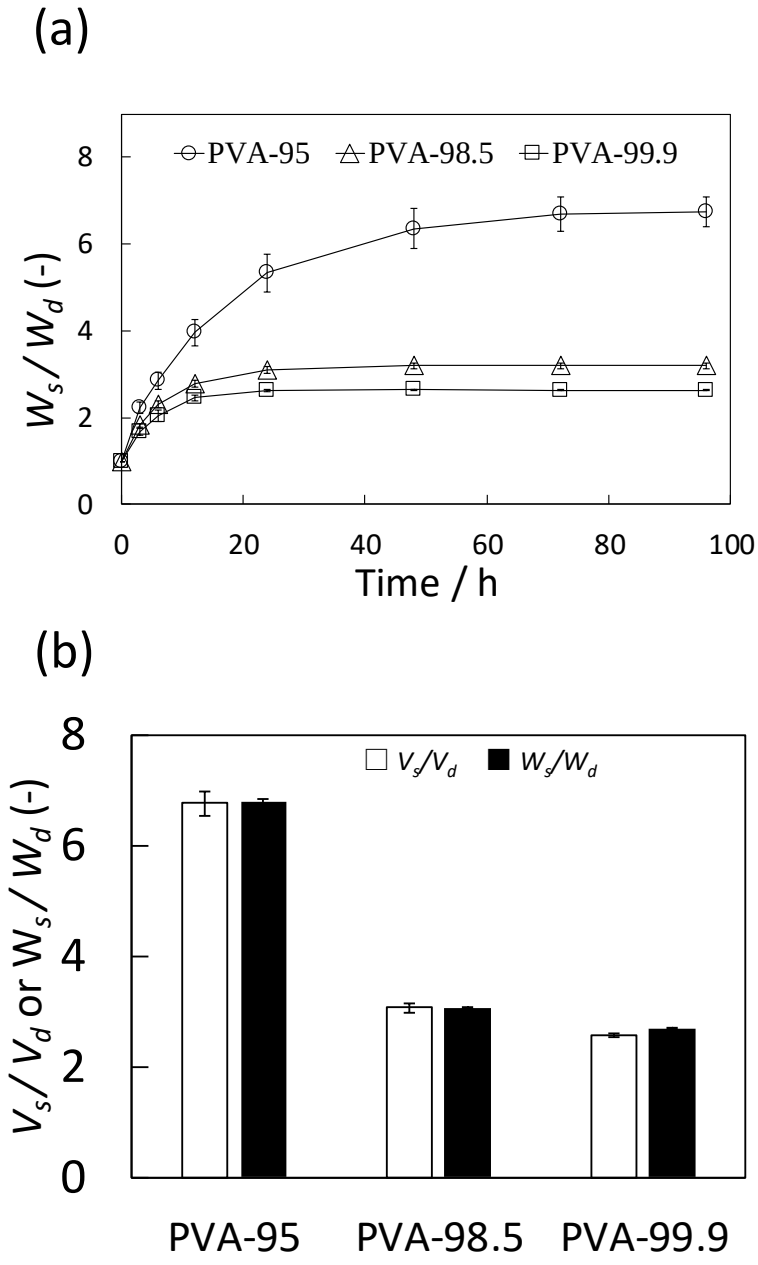
(a)
PVA-95
PVA-98.5
PVA-99.9
W_s / W_d (-)
Time / h
(b)
V_s/V_d
W_s/W_d
V_s / V_d or W_s / W_d (-)
PVA-95
PVA-98.5
PVA-99.9

Figure 2

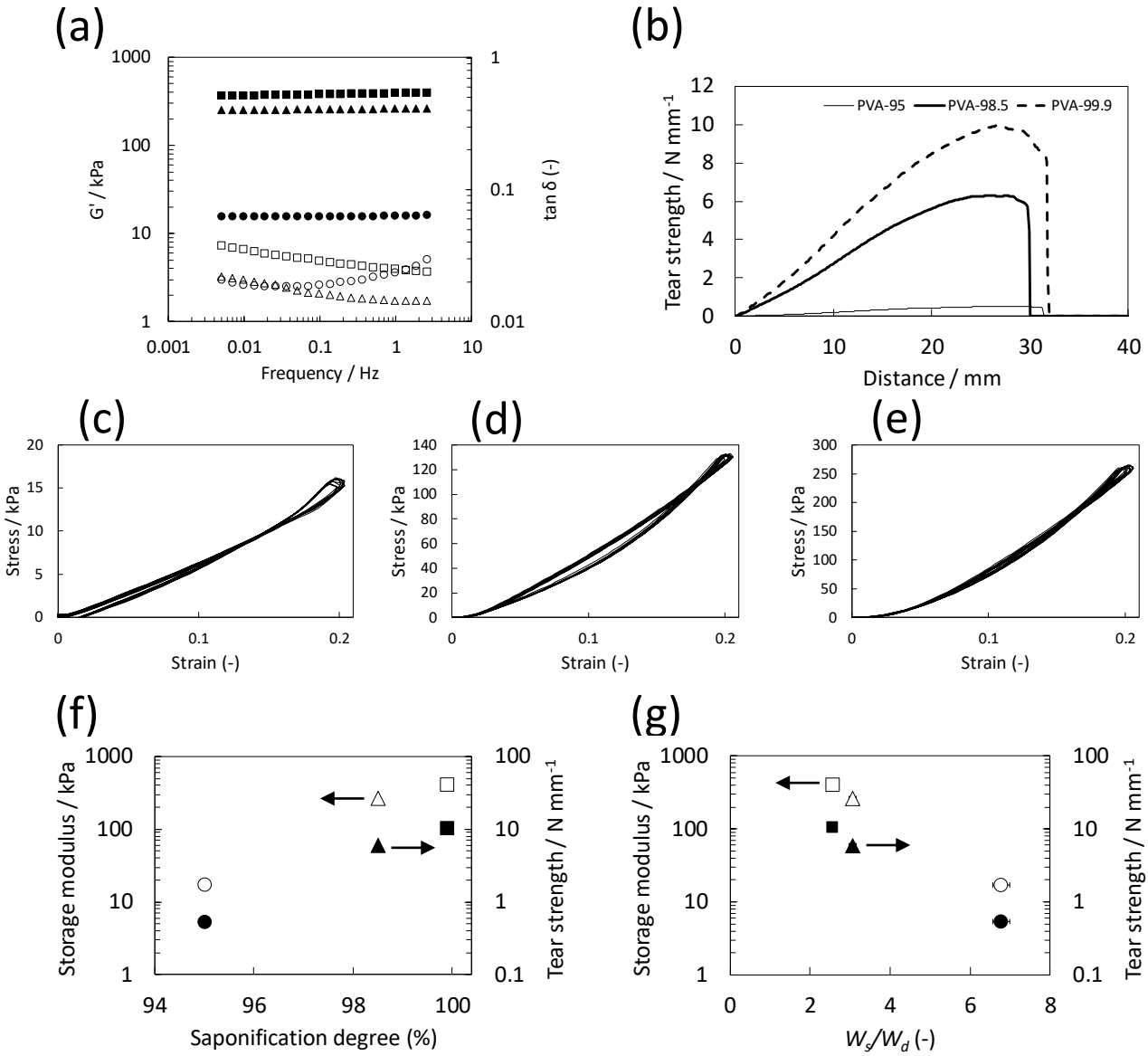
(a)
G' / kPa
tan δ (-)
Frequency / Hz
(b)
Tear strength / N mm-1
PVA-95
PVA-98.5
PVA-99.9
Distance / mm
(c)
(d)
(e)
Stress / kPa
Strain (-)
(f)
Storage modulus / kPa
Tear strength / N mm-1
Saponification degree (%)
(g)
Storage modulus / kPa
Tear strength / N mm-1
Ws/Wd (-)

Figure 3

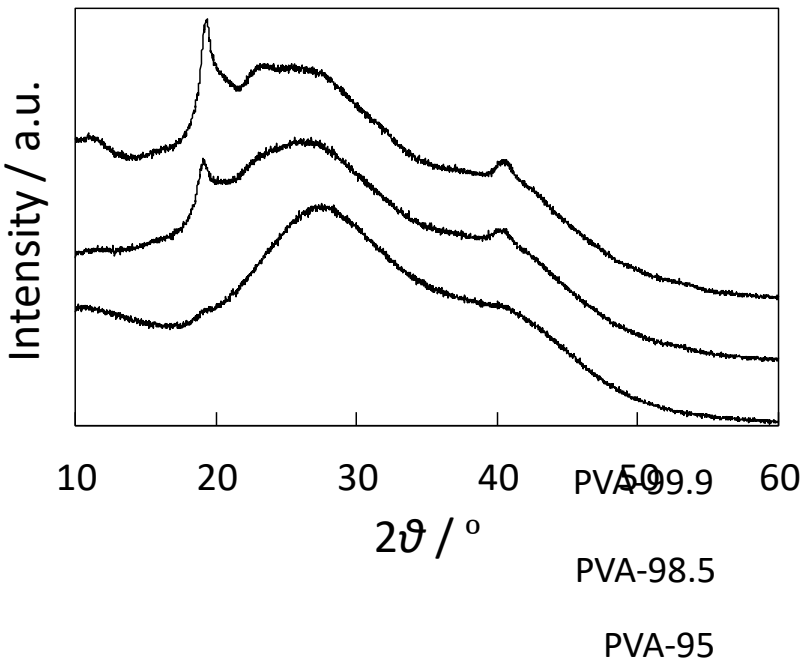

Figure 4

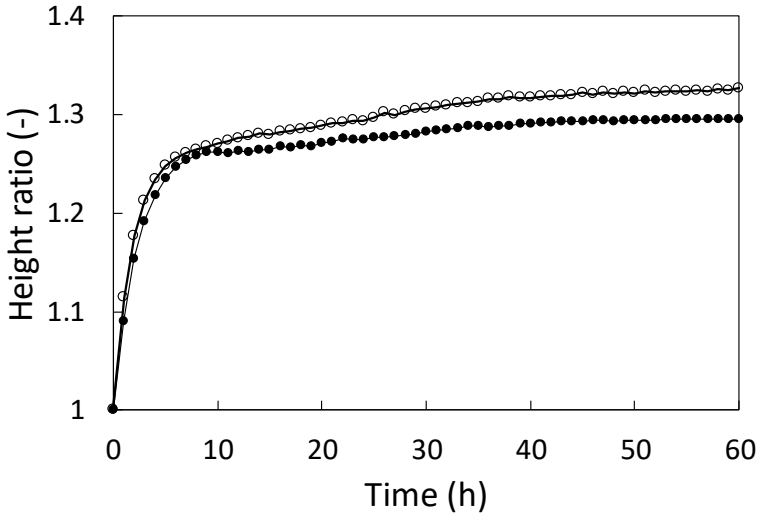

Figure 5

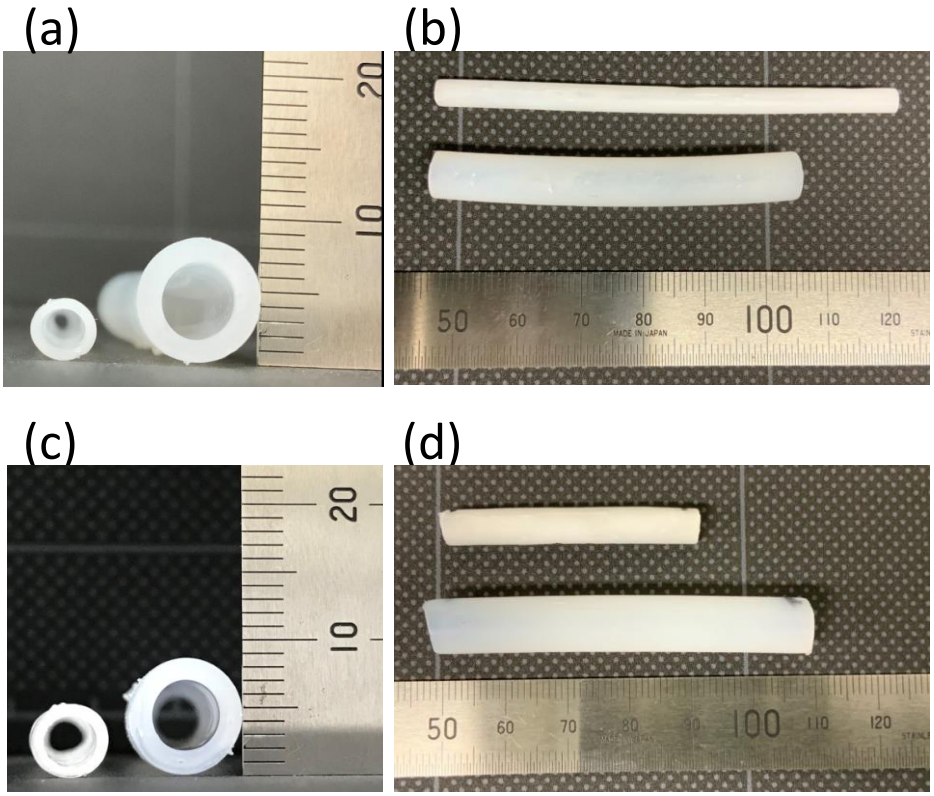

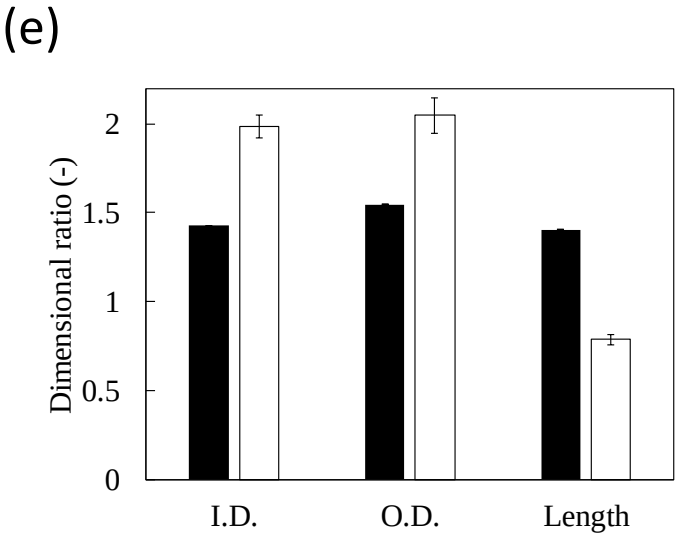

Figure 6

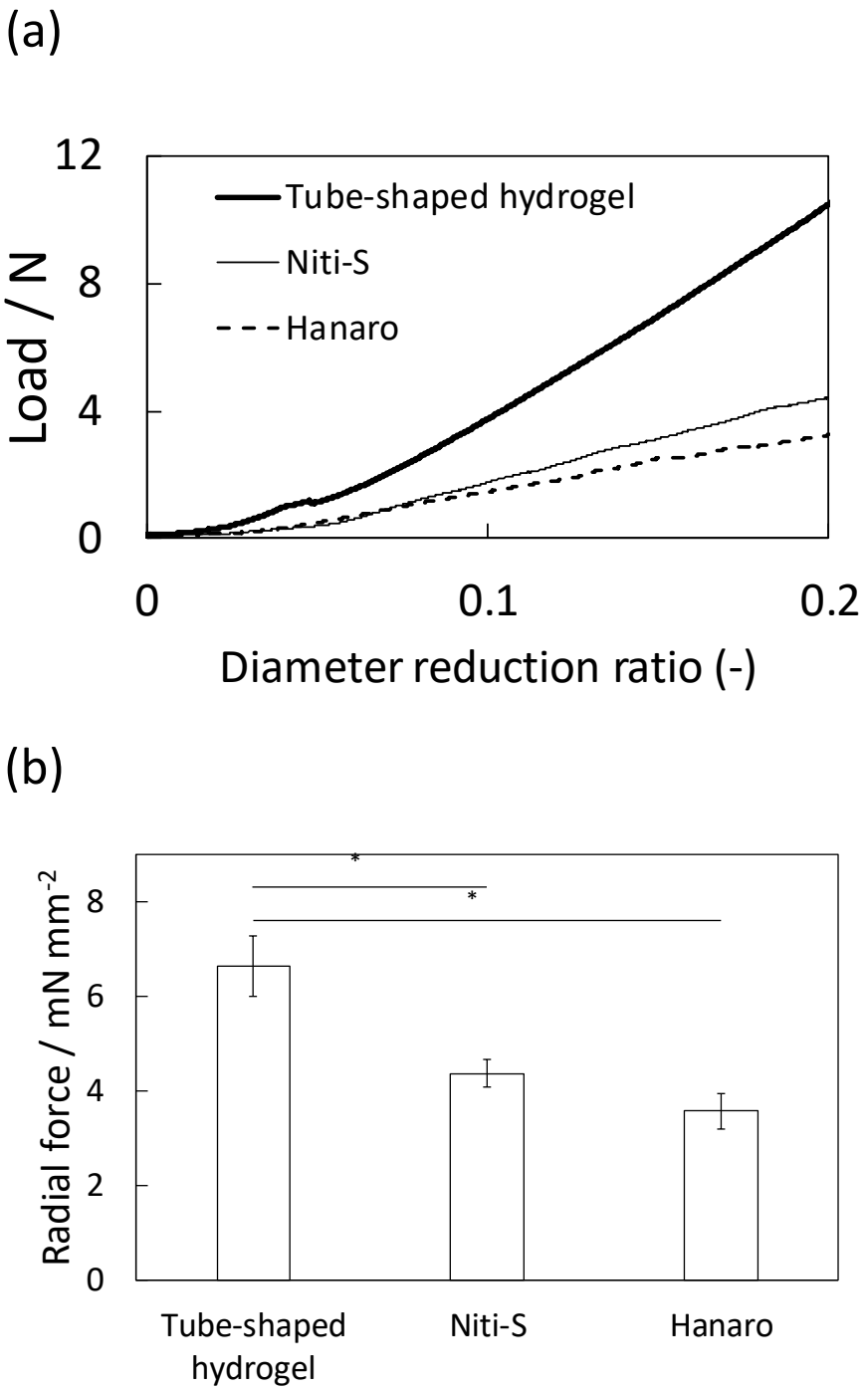
(a)
12
8
4
0
Load / N
Tube-shaped hydrogel
Niti-S
Hanaro
0
0.1
0.2
Diameter reduction ratio (-)
(b)
Radial force / mN mm-2
8
6
4
2
0
*
*
Tube-shaped hydrogel
Niti-S
Hanaro